Shahrood University of Technology

Journal of Mining and Environment (JME)

Journal homepage: www.jme.shahroodut.ac.ir

Iranian Society of Mining Engineering (IRSME)

Geochemical Speciation, Pollution Level and Health Risk Assessment of Potentially Toxic Elements in Sungun Porphyry Copper Tailings

Ali Najmeddin*, Taha Salahjou, and Kimia Zendehdel

School of Mining Engineering, College of Engineering, University of Tehran, Tehran, Iran

Article Info

Received 15 November 2025
Received in Revised form 26 December 2025
Accepted 19 January 2026
Published online 19 January 2026

DOI: 10.22044/jme.2026.17152.3391

Keywords

Mine Tailings
Health Risk Assessment
Chemical Speciation
Geochemical Fractionation
Sungun Mine

Abstract

Porphyry copper mining generates substantial volumes of tailings, which pose considerable environmental and public health hazards due to their capacity for acid generation and the release of potentially toxic elements (PTEs). This study provides an integrated environmental and human health risk assessment of tailings from the Sungun porphyry copper mine in northwestern Iran. A comprehensive and multidisciplinary approach was employed, combining physicochemical, mineralogical and geochemical analyses with statistical methods. Chemical speciation was done by employing a modified procedure suggested by the BCR (European Community Bureau of Reference) which has also been used in numerous studies to assess the geochemical fractionation and mobility of elements. The main goal was to advance from total concentration analysis to a more precise, bioavailability-based risk evaluation utilizing the USEPA framework for both children and adults. Mineralogical investigation indicated a net acid-generating capability, with pyrite content (~4%) typically surpassing that of the principal neutralizing mineral, calcite (~2%). Geochemical analyses verified that the tailings exhibit significant enrichment in Cu and Mo, along with moderate enrichment of As and Co. Among the studied elements, the highest mobility factors belonged to Cu (81.49%), Pb (76.71%), Zn (71.65%) and Mo (59.27%), respectively. The non-carcinogenic hazard index (HI) for children was 2.04, exceeding the safety threshold of 1.0, with bioavailable vanadium recognized as the principal risk factor. These findings highlight that relying solely on total PTE concentrations can be misleading, reinforcing the need for speciation-based assessments to accurately characterize the environmental behaviour and health risks of mine tailings.

1. Introduction

The increasing global demand for base metals, particularly copper (Cu), is intrinsically linked to the generation of significant quantities of finely ground mine tailings, which constitute one of the most critical environmental hazards of modern mining [1]. Porphyry-copper systems, which provide the majority of the world's copper, are often low-grade; thus, over 99% of extracted ore is discarded as waste and deposited in extensive tailings storage facilities (TSFs) or dams [2]. The principal environmental hazard posed by these tailings stems from their physicochemical composition: they frequently contain residual sulfide minerals, particularly pyrite (FeS_2), which oxidize when exposed to oxygen and water, resulting in the formation of sulfuric acid [3]. Acid mine drainage (AMD/ARD) mobilizes a range of potentially toxic elements (PTEs), particularly arsenic (As), lead (Pb), cadmium (Cd), zinc (Zn) and copper (Cu), resulting in prolonged effects on

Corresponding author: najmeddinali@ut.ac.ir (A. Najmeddin)

soils and water and increasing human health hazards through ingestion, inhalation of dust and dermal exposure [4].

The Sungun porphyry copper mine produces substantial amounts of tailings that provide major environmental and human health hazards due to high levels of potentially toxic elements (PTEs) such as As, Cd, Cu, Pb and Zn [5]. These PTEs are found in concentrations that frequently exceed standard regulatory thresholds, leading to significant ecological and pollution concerns [6,7]. Therefore, a comprehensive risk assessment that accounts for the chemical speciation of these elements is essential for comprehending their mobility, bioavailability, and overall impact. The high concentrations of PTEs within the tailings primarily drive the environmental risks [3]. Geo-accumulation and potential ecological risk indices indicate severe to moderate pollution levels, with elements like Cu, As and Pb being the main contributors [6,7]. The ecological risk is significantly intensified by the chemical speciation of these elements. Sequential extraction processes indicate that certain metals are firmly bound within the tailing matrix, whilst others, notably cadmium, demonstrate considerable mobility and bioavailability, hence amplifying their risk to local aquatic environments [7]. Over time, the oxidation of sulfide minerals in these fresh sediments can release contaminants in soluble forms, posing a long-term threat to water quality and benthic organisms [8,9].

Transitioning from ecological to human health implications, exposure pathways for nearby communities include oral ingestion, dermal contact and inhalation of contaminated dust and soil [10]. Health risk assessments indicate that for most elements, the non-carcinogenic risk index for both adults and children remain below the threshold of 1, suggesting a non-significant immediate risk; however, exceptions exist for arsenic and iron in children [11]. In contrast, the carcinogenic risk reveals a more concerning scenario. Long-term exposure, especially for children, indicates a significant carcinogenic risk primarily associated with arsenic [5,12]. Oral ingestion is consistently identified as the primary exposure pathway for both non-carcinogenic and carcinogenic risks, meaning there is an urgent need to prevent the ingestion of contaminated materials [13,14].

The management and mitigation of these multifaceted risks necessitate a comprehensive strategy. The significant environmental risk potential of the tailings underscores the imperative for proper storage facilities to prevent the release of PTEs into the surrounding environment [3]. Furthermore, continuous monitoring and targeted remediation efforts are essential. These efforts must account for the speciation of contaminants, addressing the mobility and bioavailability of PTEs to effectively reduce their ecological and health impacts [15]. In conclusion, the Sungun porphyry copper tailings represent a substantial source of pollution, necessitating robust, scientifically informed management and remediation strategies to mitigate the ongoing environmental and public health threats.

The primary objective of this study is to conduct a comprehensive environmental impact and human health risk evaluation of Sungun tailings, emphasizing a mechanistic comprehension of sources, behaviour, and effects, rather than only quantifying pollutants. This study aims to: (1) examine critical physicochemical and mineralogical parameters, including particle size and key reactive phases; (2) analyse the interrelations and pollution levels of As, Co, Cr, Cu, Fe, Mo, Pb, Sc, V, and Zn in surface tailing samples; (3) assess chemical speciation and the health risks posed by these elements to both children and adults.

2. Methods/Methodology

2.1. Site Description and Geological Setting

The Sungun porphyry copper deposit is located in East-Azerbaijan province, northwestern Iran, approximately 30 km northeast of Varzeqan (Figure 1). The mine is situated in the Urumieh–Dokhtar Magmatic Assemblage (UDMA), a prominent Tertiary volcanic-plutonic belt that constitutes one of Iran's most important metallogenic provinces. The geology of the study area is defined by post-collisional calc-alkaline magmatism linked to the Alpine-Himalayan orogeny [16]. The mineralization in Sungun is predominantly contained between Miocene porphyritic andesite to monzonite intrusions that intruded Eocene volcanic country rocks, comprising trachyandesite, dacite and Andesite units (Fig. 1). Economic mineralization directly results from magmatic-hydrothermal processes [17]. Hydrothermal fluids, laden with metals and sulfur, traversed fracture networks, resulting in the deposition of various sulfide minerals. The principal ore mineralogy is characterized by chalcopyrite ($CuFeS_2$) and pyrite (FeS_2), accompanied by lesser amounts of molybdenite (MoS_2), bornite (Cu_5FeS_4), sphalerite (ZnS) and galena (PbS) [18]. The sulfide minerals are the

primary sources of the potentially toxic elements (PTEs) examined in this study. The host rocks have seen significant hydrothermal alteration, leading to a distinct zonation pattern characteristic of porphyry copper systems. This pattern, extending from a central potassic zone outward through phyllic, argillic and propylitic zones, has determined the creation of the corresponding gangue mineralogy. Prominent silicate and alteration minerals comprise potassium feldspar, biotite, quartz, sericite, chlorite and epidote, which form the majority of the processed tailings material [19]. The tailings produced by the ore concentrator plant are deposited in an extensive, 1,400-hectare rockfill tailings storage facility (TSF) including a clay core, situated adjacent to the mine complex (Figure 1). Established in 2006, this facility serves as the primary source of the materials examined in this research.

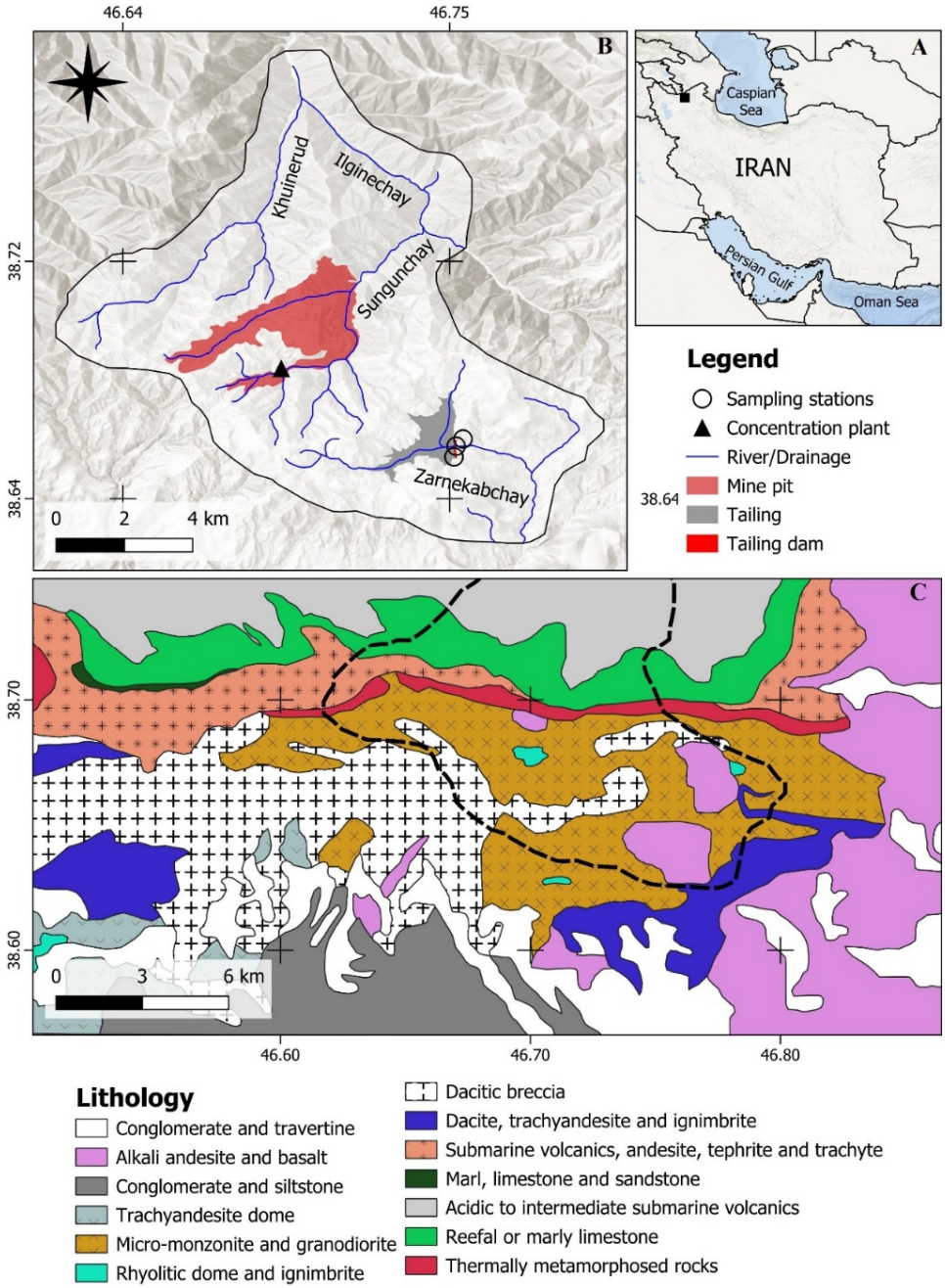

Figure 1. Location and geological map of the Sungun copper mine [20,21]. (A) Location map of the study area in East-Azerbaijan province; (B) Map of the study area showing sampling stations, mine pit and tailing dam; and (C) Geological map of the Sungun copper mine.

2.2. Sampling strategy and sample preparation

A meticulous sampling campaign was conducted in the autumn of 2023 to collect representative material. Due to the heterogeneous deposition history of the tailings, strict grid-based sampling was considered impractical. A strategic judgmental random sampling method was employed. Three surface sediment samples (0-10 cm) were obtained at different locations from a designated TSF site, encapsulated in inert polyethylene and promptly sealed. A laboratory composite (Sun-Drs-Mix) was created by homogenizing proportional aliquots from the three primary sources to accurately replicate the sampled location. Samples were managed to reduce oxidation or contamination. A GPS device was used to record the coordinates of the sampling points. The sediment samples were air-dried at room temperature in the laboratory. Next, each sample was passed through a 2-mm nylon sieve and then divided into two fractions. The initial fraction was utilized for physicochemical and mineralogical investigations, whilst the subsequent portion was subjected to a 63-µm screen (220 mesh) to isolate silt and clay fractions, enabling the determination of the total concentration of PTEs.

2.3. Analytical methods

A multi-technique analytical approach was adopted to fully characterize the physical, mineralogical and chemical properties of the tailings.

2.3.1. Mineralogical Analysis (X-ray Diffraction - XRD)

The bulk mineralogy was analyzed using powder X-ray diffraction (XRD) at a commercial laboratory (Kansaran Binaloud, Iran). Back-loaded holders reduced preferred orientation; scans utilized Cu Kα radiation (λ = 1.5406 Å) at 40 kV, 30 mA, with 2θ = 5–70°, a step size of 0.02° and a dwell time of 1–2 s per step. Diffraction patterns were analyzed with High Score Plus in comparison to the ICDD PDF 4 database. Semi-quantitative phase proportions were assessed by Rietveld refinement and/or Reference Intensity Ratios, utilizing internal corundum standard validations when applicable. For samples exhibiting distinct clay halos, a <2 µm clay fraction was obtained using sedimentation; oriented mounts were examined in air-dried, glycolated (with ethylene glycol) and heated (at 550 °C) states to differentiate between smectite, illite, kaolinite and chlorite interlayers. XRD identified sulfide and sulfate phases (e.g., pyrite, chalcopyrite, gypsum) relevant to acid production and trace element mobility.

2.3.2. Major Oxides

The bulk elemental composition of the tailings was determined by X-ray Fluorescence (XRF) spectrometry. Samples were prepared as fused lithium borate beads to minimize mineralogical and particle size effects. The analysis was conducted using a wavelength-dispersive XRF spectrometer (e.g., PANalytical Axios Max) at Kansaran Binaloud Laboratory, providing quantitative data for major oxides (SiO_2, Al_2O_3, Fe_2O_3, CaO, MgO, Na_2O, K_2O, P_2O_5, TiO_2, MnO) and trace elements.

2.3.3. Particle Size Distribution

Particle-size distributions were ascertained using laser diffraction (e.g., Mastersizer-class device) on oven-dried material (<2 mm). Representative subsamples were suspended in isopropanol and subjected to brief ultrasonication to reduce agglomeration; refractive indices were configured according to manufacturer defaults for silicates. Repetitive trials guaranteed consistency (±3% for D50). D50, D80 and D90 were documented and utilized to contextualize mineral-phase distribution over size fractions.

2.3.4. Trace Element Analysis

To accurately quantify trace and minor elements, including potentially toxic elements (PTEs), samples underwent digestion with a potent multi-acid mixture (HNO_3-HCl-HF-$HClO_4$) to ensure near-total dissolution, followed by analysis using inductively coupled plasma optical emission spectrometry (ICP-OES, PerkinElmer Optima-class) for PTE totals (As, Co, Cr, Cu, Fe, Mo, Pb, Sc, V, and Zn). Elemental analysis was performed on 37 elements at the Kansaran Binaloud Laboratory in Iran. This study concentrates on 10 priority pollutants as designated by the United States Environmental Protection Agency (USEPA). Calibration utilized certified multi-element standard solutions and quality assurance/quality control (QA/QC) processes, including the analysis of procedural blanks and certified reference materials (CRMs), were strictly followed to guarantee data correctness and precision.

2.3.5.BCR Sequential Extraction for Chemical Speciation

The chemical speciation of potentially toxic elements (PTEs) was assessed utilizing the three-

stage BCR sequential extraction process, which separates elements into three mobile forms, followed by a fourth step to ascertain the residual fraction. The procedures were:

- Step 1: F1 (Acid-soluble/Exchangeable Fraction): Extraction with 0.11 M acetic acid.
- Step 2: F2 (Reducible Fraction): Extraction of the residue from Step 1 with 0.5 M hydroxylamine hydrochloride (pH 1.5).
- Step 3: F3 (Oxidizable Fraction): Digestion of the residue from Step 2 with 8.8 M hydrogen peroxide, followed by extraction with 1.0 M ammonium acetate (pH 2.0).
- Step 4: R (Residual Fraction): Complete digestion of the final residue using aqua regia.

Following each of the initial three procedures, the mixture underwent centrifugation, the supernatant was decanted for analysis and the residue was rinsed prior to the subsequent step. The concentrations of Co, Cr, Cu, Fe, Mo, Pb, Sc, V and Zn in the supernatant from each of the four stages were quantified using ICP-OES at Kansaran Binaloud Laboratory, Iran. To evaluate the accuracy of the sequential extraction results in the TSF samples, the recovery percentage (% R) was also computed as follows:

$$\text{Recovery (\%)} = \frac{F_1 + F_2 + F_3 + R}{TC} \times 100 \quad (1)$$

Where, F1, F2, F3, R and TC indicate the concentration extracted in each fraction and the pseudo-total concentration of PTEs, respectively. In this study, the recovery values of all PTEs (except for As) range from 98% to 119% showing a good accordance between total concentrations and the sum of fractions. Hence, As was excluded from the sequential extraction analyses. The high recovery value for this element is the result of the very low concentrations analysed for some samples and thus, they cannot affect the results considerably [22].

2.4. Environmental and Health Risk Assessment

2.4.1. Pollution Intensity Assessment

The Enrichment Factor (EF) was computed for each potentially toxic element (PTE) to measure the extent of elemental enrichment in the tailings compared to natural background values. The EF standardizes the concentration of a target element relative to a conservative, lithogenic reference element to differentiate between natural geological changes and anthropogenic impacts from mining and processing activities. The EF was computed utilizing the subsequent equation:

$$EF = \frac{([C_x]/[C_{\text{ref}}])_{\text{sample}}}{([C_x]/[C_{\text{ref}}])_{\text{background}}} \quad (2)$$

where ($[C_x]/[C_{ref}]$) sample is the ratio of the concentration of the element of interest (C_x) to the concentration of the reference element (C_{ref}) in the tailings sample and ($[C_x]/[C_{ref}]$) background is the same ratio in a defined background material [22]. This study designated Scandium (Sc) as the reference element following a thorough statistical assessment. Sc exhibits a pronounced lithogenic origin, elevated geochemical stability, little vulnerability to anthropogenic contamination and low variability among samples. Pearson correlation study established a robust positive association between Sc and other immobile lithogenic elements (Fe, Al, Ti, Zr), affirming its appropriateness. To guarantee worldwide comparability of results, the mean elements concentrations in world soils, as documented by authoritative geological databases [23], were utilized as the background values (B_x and B_{ref}).

2.4.2. Human Health Risk Assessment

A screening-level Human Health Risk Assessment (HHRA) was performed to deliver an initial estimation of the possible non-carcinogenic and carcinogenic risks to human health from direct contact to the tailings material. This assessment does not measure actual exposure but rather assesses the potential risk posed by the tailings as a source medium, utilizing plausible direct contact scenarios. The risk assessments were based on the bioavailable concentration of each element, defined as the sum of the mobile fractions (F1+F2+F3) identified during the BCR sequential extraction, to provide a more precise estimation of potential health impacts, instead of depending on the total concentration. This method conforms to best practices, as only the non-residual, labile fraction of an element is anticipated to be assimilated by human receptors after unintentional consumption. The methodology was founded on the principles and models established by the United States Environmental Protection Agency (USEPA) [24]. The evaluation examined three main exposure routes: (1) inadvertent intake of tailings particles, (2) inhalation of fugitive dust produced from the tailings surface and (3) direct skin contact with the material. Risks were assessed independently for two vulnerable receptor groups: children (ages 1–

6) and adults (ages >6), to consider variations in their physiology and behaviour.

2.4.2.1. Non-Carcinogenic Risk Assessment

The potential for adverse non-carcinogenic health effects was evaluated by calculating the Hazard Quotient (HQ) for each element and exposure pathway. The HQ is the ratio of the estimated exposure, or Average Daily Dose (ADD), to the reference dose (R_fD), which is the level of daily exposure considered safe over a lifetime.

The ADD (in mg/kg-day) for each pathway was calculated using the following standard USEPA equations:

$$ADD_{\text{ing}} = \frac{C \times IngR \times EF \times ED}{BW \times AT} \times CF \quad (3)$$

$$ADD_{\text{inh}} = \frac{C \times InhR \times EF \times ED}{PEF \times BW \times AT} \quad (4)$$

$$ADD_{\text{derm}} = \frac{C \times SA \times AF \times ABS \times EF \times ED}{BW \times AT} \times CF \quad (5)$$

The Hazard Quotient for each element (i) and pathway (j) was then calculated as:

$$HQ_{i,j} = \frac{ADD_{i,j}}{RfD_{i,j}} \quad (6)$$

To assess the cumulative potential for non-carcinogenic effects from all contaminants and pathways, the Hazard Index (HI) was calculated as the sum of all individual HQs:

$$HI = \sum_{i=1}^{n} \left(HQ_{i,ing} + HQ_{i,inh} + HQ_{i,\text{derm}}\right) \quad (7)$$

An HI value less than 1.0 suggests that adverse non-carcinogenic health effects are unlikely to occur, whereas an HI value greater than 1.0 indicates a potential for health concerns, warranting further investigation.

2.4.2.2. Carcinogenic Risk Assessment

The potential for carcinogenic risk was estimated for elements classified as known or suspected human carcinogens by the USEPA (e.g., As, Co, Cr, Pb). The risk is expressed as the Incremental Lifetime Cancer Risk (ILCR), which is the probability of an individual developing cancer over a lifetime due to exposure [25]. The ILCR was calculated based on the Lifetime Average Daily Dose (LADD), which is determined using the same formulas as the ADD (Equations 3–5), but with the averaging time (AT) specifically set to a 70-year lifetime (70 years × 365 days/year). The ILCR for each carcinogen (i) and pathway (j) was then calculated using the corresponding Cancer Slope Factor (CSF):

$$ILCR_{i,j} = LADD_{i,j} \times CSF_{i,j} \quad (8)$$

The total cancer risk is the sum of the ILCR values across all carcinogenic elements and all exposure pathways. According to USEPA guidelines, an ILCR below 1×10^{-6} is considered negligible, while a risk above 1×10^{-4} is generally considered unacceptable and may trigger regulatory action. The exposure parameters used in the HHRA calculations for both child and adult receptors are detailed in Table 1.

Table 1. Exposure Parameters Used in the Human Health Risk Assessment Model

Parameter	Symbol	Definition	Unit	Child	Adult	Source
Concentration	C	F1 + F2 + F3	mg/kg	Measured	Measured	This Study
Ingestion Rate	IngR	Rate of incidental dust ingestion	mg/day	200	100	[25]
Inhalation Rate	InhR	Rate of air inhalation	m³/day	10	20	[25]
Exposure Frequency	EF	Frequency of exposure events	days/year	350	350	[25]
Exposure Duration	ED	Duration of exposure period	years	6	24	[25]
Body Weight	BW	Average body weight	kg	15	80	[25]
Averaging Time (Non-carcinogenic)	AT_nc_	Period over which exposure is averaged	days	ED × 365	ED × 365	[25]
Averaging Time (Carcinogenic)	AT_c_	Lifetime period for averaging exposure	days	70 × 365	70 × 365	[25]
Skin Surface Area	SA	Exposed skin area	cm²/day	2800	5700	[24]
Adherence Factor	AF	Soil adherence to skin	mg/cm²	0.2	0.07	[25]
Dermal Absorption Factor	ABS	Fraction of element absorbed via skin	unitless	0.001	0.001	[24]
Particulate Emission Factor	PEF	Emission factor for airborne particles	m³/kg	1.36×10^9	1.36×10^9	[24]

2.5. Statistical Analysis

All statistical analyses of the geochemical data were conducted utilizing IBM SPSS Statistics software (version 28). A range of statistical techniques was utilized to examine inter-element connections, ascertain geochemical linkages and facilitate the interpretation of the environmental assessment findings. Descriptive statistics, including mean, median, standard deviation, minimum, and maximum values, were calculated for the concentrations of all analysed elements. Box plots were utilized to illustrate the distribution of EF values for principal PTEs. This graphical method was selected for its capacity to effectively illustrate the central tendency (median), dispersion (interquartile range) and skewness of the data, while also identifying potential outliers that may signify severe enrichment. A Pearson correlation matrix was constructed to analyse the relationships among the variables. The Pearson correlation coefficient (r) was employed to assess the strength and direction of the linear relationship between pairs of elemental concentrations. This analysis was essential in identifying elements exhibiting similar geochemical behaviours (e.g., those linked to sulfide mineralization versus those linked to silicate gangue) and offered a strong statistical rationale for selecting Scandium (Sc) as the lithogenic reference element for the EF calculations. Additionally, Hierarchical Cluster Analysis (HCA) was utilized to categorize the elements according to their statistical similarities, offering further evidence for their possible common origins. The technique utilized Euclidean distance to assess similarity across elements and using Ward's linking method for cluster formation. The HCA results were depicted as a dendrogram, which graphically represents the structure of elemental groupings and their levels of relationship.

3. Results and discussion

3.1. Mineralogical Composition, Physical Properties and Geochemical Characterization of Tailings

The essential solid-phase properties of the tailings were determined using X-ray diffraction and laser particle size characterization, as these parameters govern the material's geochemical reactivity, hydraulic behaviour and potential for pollutant mobilization. In addition, the elemental composition of the tailings was analysed to quantify both matrix-forming elements and environmentally significant trace elements, providing a comprehensive understanding of their chemical and physical characteristics.

3.1.1. Mineralogical Assemblage

The mineralogical composition of the four tailing samples (Sun-Drs-1, Sun-Drs-2, Sun-Drs-3 and Sun-Drs-mix), as ascertained using semi-quantitative X-ray Diffraction (XRD) analysis, is presented in Table 2. The four XRD datasets indicate that, within the specific horizon and time window sampled, quartz (45–47%), illite (20–21%), orthoclase (11–12%), albite (10%), pyrite (4%), kaolinite (3%) and calcite (2%) show very low inter-sample variance (CV ≤ 4.3%; Figure 3). This statistical uniformity reflects stable mill feed and operating conditions during the short sampling campaign but does not capture the full vertical and temporal heterogeneity that typically characterizes large porphyry tailings storage facilities.

This mineral assemblage clearly signifies byproducts derived from porphyry copper deposits. These deposits are inherently linked to modified felsic to intermediate intrusive rocks, including granodiorite and quartz monzonite, characterized by high concentrations of quartz and feldspars (orthoclase and albite). Illite, a mica-group clay mineral, indicates sericite, a defining feature of the phyllic (quartz-sericite-pyrite) alteration zone, which is essential in the spatial and genetic models of several porphyry copper systems. The primary silicate minerals (quartz, orthoclase, albite) have significant stability and constitute the main gangue matrix of the tailings. The simultaneous presence of pyrite (FeS_2) and calcite ($CaCO_3$) is of notable environmental importance. Pyrite, an iron sulfide mineral, is the primary catalyst of acid mine drainage (AMD). The oxidation of sulfur in the presence of ambient oxygen and water produces sulfuric acid, significantly reducing the pH of leachate and receiving waters, thus enhancing the mobility and bioavailability of heavy metals. In contrast, calcite functions as a primary acid-neutralizing agent. It promptly interacts with and neutralizes hydrogen ions (H^+), stabilizing the system's pH and alleviating the emergence of acidic circumstances. The enduring geochemical stability of mine tailings is frequently determined by the equilibrium between their acid-generating capacity (associated with pyrite content) and their acid-neutralizing capacity (mostly derived from calcite and other carbonate minerals). In the Sungun tailing samples, the relative abundance of pyrite (about 4%) is consistently double that of calcite (approximately 2%). This mismatch

indicates that although the tailings have a certain buffering capacity, it is probably inadequate to neutralize all the acid produced by the total oxidation of pyrite. The tailings exhibit a prolonged net acid-generating potential, posing a latent environmental risk until the more reactive calcite is depleted.

Table 2. Mineralogical Composition (%) of Tailing Samples by XRD

Mineral	Chemical Formula	Sun-Drs-1	Sun-Drs-2	Sun-Drs-3	Sun-Drs-mix
Quartz	SiO_2	45	47	45	46
Illite	$KAl_2(Si_3Al)O_{10}(OH)_2$	21	20	21	21
Orthoclase	$KAlSi_3O_8$	12	11	12	11
Albite	$NaAlSi_3O_8$	10	10	10	10
Pyrite	FeS_2	4	4	4	4
Kaolinite	$Al_2Si_2O_5(OH)_4$	3	3	3	3
Calcite	$CaCO_3$	2	2	2	2

Figure 2 illustrates that all four samples include a silicate-dominated matrix, comprising around 45–47% quartz, 20–22% illite/sericite, 11–12% orthoclase and 9–10% albite. Minor accessories include approximately 4% pyrite, 3% kaolinite and 2% calcite, suggesting a restricted carbonate buffering capacity in comparison to acid-generating sulfides. The relative stability of phase proportions among Sun-Drs-1/2/3 and the mixed composite substantiates the application of a unified geochemical model for the deposit's fine waste stream. The pyrite to calcite ratio is crucial for environmental stability; prolonged oxidation would exceed neutralization, leading to increased acidity and the mobilization of redox-sensitive trace elements. The mineralogical controls delineate the reactivity patterns and exposure processes assessed in the next sections and serve as validations for XRF and speciation outcomes.

Calculation of phase-specific statistical variance across four XRD datasets allowed for the quantification of inter-sample variability. Quartz presented a mean of 45.75 ± 0.96% (CV = 2.1%). Illite followed with 20.5 ± 0.5% (CV = 2.4%); orthoclase recorded 11.5 ± 0.5% (CV = 4.3%). Albite and pyrite exhibited zero variance. Albite remained at 10.0 ± 0.0% (CV = 0%). Pyrite measured 4.0 ± 0.0% (CV = 0%). Kaolinite (3.0 ± 0.0%) and calcite (2.0 ± 0.0%) showed similar stability. These low coefficients of variation signal minimal phase heterogeneity within the specific sampled horizon. This uniformity does not preclude the vertical or operational variability typical of porphyry tailings systems. To further illustrate the degree of mineralogical uniformity among the analysed tailings samples, the mean phase proportions and their corresponding standard deviations were visualized. Figure 3 provides a statistical representation of inter-sample variance, supporting the observation that quartz, illite and feldspar phases exhibit low variability across the four XRD measurements. Although this stability likely reflects consistent mill feed conditions during the sampling interval, it does not preclude broader heterogeneity within the tailing's facility. These low coefficients of variation therefore quantify the degree of local compositional reproducibility among the four subsamples. However, they should be interpreted as phase-specific statistics for a limited spatial and temporal window, not as evidence that the entire Sungun TSF is compositionally uniform.

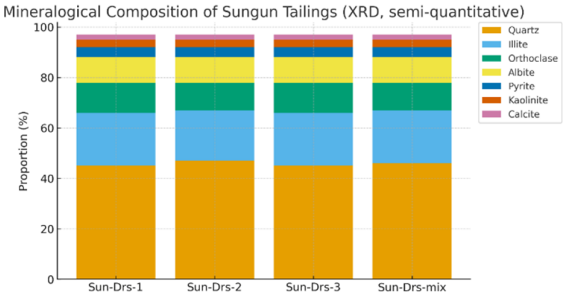

Figure 2. Semi-quantitative XRD mineralogy of four tailing samples. Pyrite exceeds calcite in all samples, indicating a net acid-generating tendency.

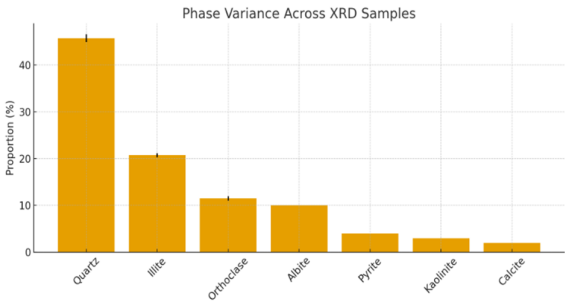

Figure 3. Statistical variance of XRD-derived mineral phases across the four tailings samples. Bars represent mean mineral proportions and error bars denote one standard deviation.

The equilibrium between the acid-producing potential (APP), mainly derived from pyrite and the acid-neutralizing potential (ANP), predominantly sourced from calcite, is a crucial factor influencing the environmental behaviour of tailings. In the examined samples, the relative abundance of pyrite (~4%) is consistently twice that of calcite (~2%). This disparity indicates that although the tailings have an initial intrinsic buffering capacity, there exists a net potential for acid formation in the long term. Upon the depletion of the more reactive calcite due to continuous pyrite oxidation, the system's pH is expected to decline, potentially triggering acid mine drainage (AMD) and enhancing the mobility of associated potentially hazardous components. 1 This mineralogical composition suggests a substantial environmental danger that necessitates meticulous control.

3.1.2. Major Oxides

The comprehensive chemical composition of the tailing samples, determined using X-ray Fluorescence (XRF) spectrometry, is presented in Table 3. The data indicates that the tailings are mostly composed of silica (SiO_2), with concentrations varying from 66.22 wt.% to 69.75 wt.% and alumina (Al_2O_3), with concentrations ranging from 12.25 wt.% to 13.60 wt.%. Other notable constituents comprise iron oxide (Fe_2O_3, 4.14–4.35 wt.%) and potassium oxide (K_2O, 4.20–4.65 wt.%). The Loss on Ignition (LOI), indicative of volatile constituents including water from hydrous minerals, carbonates and organic matter, ranged from 4.47% in the mixed sample to a maximum of 8.21% in sample Sun-Drs-3.

The main oxide data strongly corroborate the mineralogical assemblage revealed by XRD. The elevated levels of SiO_2 directly indicate the prevalence of quartz (pure SiO_2) and the silicate structure of feldspars and clay minerals. The quantified levels of Al_2O_3, K_2O and Na_2O align with the existence of K-feldspar (orthoclase), Na-feldspar (albite) and the potassium-rich clay mineral illite. The concentrations of Fe_2O_3 (expressed as total iron) and sulfur (S, 1.80–1.89 wt.%) are directly linked to the approximately 4% pyrite (FeS_2) detected in the XRD study. The calcium oxide (CaO) concentration of 1.05–1.22 wt.% corresponds with the approximately 2% calcite ($CaCO_3$) identified. The substantial consistency between the two independent analytical techniques (XRD and XRF) instils considerable confidence in the comprehensive characterization of the tailings matrix, affirming that the chemical and mineralogical data provide a coherent and unified representation of the material's composition.

Table 3. Major Oxide Composition (wt.%) of Tailing Samples by XRF

Oxide/Parameter	Sun-Drs-1	Sun-Drs-2	Sun-Drs-3	Sun-Drs-mix
SiO_2	67.08	69.34	66.22	69.75
Al_2O_3	13.60	12.25	12.95	13.02
Fe_2O_3	4.30	4.14	4.24	4.35
K_2O	4.65	4.20	4.45	4.40
Na_2O	0.91	0.91	0.89	0.93
CaO	1.19	1.05	1.22	1.19
MgO	1.30	1.24	1.23	1.30
LOI	6.29	6.31	8.21	4.47

The bulk chemistry presented in Figure 4 supports the XRD assemblage. SiO_2 predominates (~66–70 wt %) followed by Al_2O_3 at ~12–14 wt % and K_2O at ~4–5 wt %, aligning with a quartz–feldspar–mica structure. Fe_2O_3 approximately 4.1–4.4 wt % and S approximately 1.8–1.9 wt % correspond to the small yet pervasive sulfide inventory deduced from XRD, with pyrite around 4%. In contrast, the CaO content of approximately 1–1.2 wt % is consistently low, corroborating the infrequent presence of calcite and, by extension, a restricted acid-neutralizing capacity. This cross-validation enhances confidence that geochemical behaviour is dictated by silicate host phases with redox-sensitive microenvironments, rather than by prevalent carbonates, a hypothesis further explored in fractionation and mobility studies.

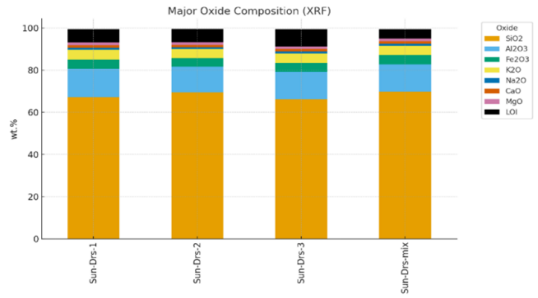

Figure 4. Stacked major-oxide compositions for the four samples, consistent with a quartz–feldspar–mica matrix and minor carbonate buffering.

3.1.3 Particle Size Distribution

The particle size analysis results, presented in Figure 5, reveal that the tailings consist of fine-grained materials, primarily comprising particles within the silt and fine sand size fractions. The median particle size (D50) ranges from 21.33 µm to 50.57 µm across the different samples. Sample Sun-Drs-1 was identified as the most finely grained material, displaying the lowest D50 (21.33 µm) and D80 (99.55 µm) values. In contrast, sample Sun-Drs-2 displayed the highest particle size, with a D50 of 50.57 µm. The composite sample (Sun-Drs-mix) demonstrated a relatively fine texture (D50 = 33.56 µm), indicating the impact of the finer constituents in the mixture.

The fine-grained texture results directly from the comminution techniques employed in mineral processing to separate rich copper and molybdenum minerals from the host rock matrix for recovery through froth flotation. The efficacy of the flotation process is significantly influenced by particle size, with optimal recovery generally attained for particles measuring between 30 and 150 µm. Ultrafine (<30 µm) and coarse (>150 µm) sulfide particles frequently demonstrate inadequate recovery, resulting in their rejection to the tailings stream, hence influencing the reported particle size distribution.

The particle size distribution is a crucial factor influencing the environmental behaviour of the tailings. The abundance of tiny particles leads to a significant specific surface area per unit mass, facilitating a broad interface for geochemical processes. The augmented surface area improves the tailings' ability to absorb dissolved metals from the solution and increases the weathering rates of minerals such as pyrite, potentially elevating the rate of acid formation. Studies on copper tailings have consistently shown that potentially harmful constituents are frequently concentrated in the finest particle size fractions. This enrichment results from surface adsorption processes and the presence of residual, unrecovered sulfide minerals as micro-inclusions within gangue particles, which are only released by fine grinding. Moreover, an increased fraction of fine particles diminishes the hydraulic conductivity of the tailings impoundment, potentially resulting in water saturation. This state may restrict oxygen entry, thereby conserving sulfides, but it can also promote swift and extensive acid production if the system is subsequently exposed to air oxygen. The fine-grained texture of the Sungun tailings elevates their environmental risk by augmenting the surface area for acid-generating reactions and enhancing the material's ability to adsorb and subsequently release contaminants under varying geochemical conditions.

Figure 5 illustrates that the tailings are consistently fine, with a D50 range of approximately 21–51 µm, a D80 range of approximately 100–125 µm and a D90 range of approximately 170–180 µm, characteristic of flotation wastes. The fineness increases the reactive surface area, hence accelerating sulfide oxidation kinetics and interaction with meteoric waters, while the D90 of around 180 µm indicates a continuous fine-sand tail susceptible to aeolian entrainment under arid, windy circumstances. Inter-sample variations are minimal; nevertheless, Sun-Drs-2 and Sun-Drs-3 exhibit a slight coarseness (elevated D50), aligning with fluctuations in grinding and classifying processes. From a risk standpoint, these grain sizes enhance the ingestion and cutaneous pathways through soil/dust transfer, while also elucidating the swift equilibration noted in the subsequent leaching and bio accessibility studies.

3.1.4 Potentially Toxic Element Concentrations

Table 4 summarizes the concentrations of ten environmentally relevant trace elements in the tailings, measured by ICP-OES analysis. The dataset has a distinct geochemical signature typical of porphyry copper systems. Copper is significantly elevated, with a mean concentration of approximately 753.8 mg kg^{-1}, nearly 50 times the global soil background level of around 14 mg kg^{-1}. Molybdenum (Mo) levels are similarly increased, with a mean of approximately 67.4 mg kg^{-1}, which is almost 37 times its background concentration of approximately 1.8 mg kg^{-1}. Excessive concentrations of many potentially deleterious elements surpass background levels, including arsenic (As, mean = 12.0 mg kg^{-1}), cobalt (Co, mean ≈ 19.3 mg kg^{-1}), lead (Pb, mean ≈ 26.8 mg kg^{-1}) and vanadium (V, mean ≈ 65.8 mg kg^{-1}). This elemental correlation aligns with tailings from a porphyry copper deposit, whereby chalcopyrite ($CuFeS_2$) and molybdenite (MoS_2) serve as the primary ore minerals, while accessory sulfides (e.g., arsenopyrite, galena, sphalerite) may introduce As, Pb and Zn. The mean copper concentration (≈ 753.8 mg kg^{-1}) exceeds the international soil guideline levels for Iran (100 mg kg^{-1}), China (100 mg kg^{-1}), Canada (91 mg kg^{-1}) and the Netherlands (36 mg kg^{-1}) by factors ranging from around 7.5 to 21. Molybdenum

surpasses regulatory limits for Iran (10 mg kg^{-1}) and Canada (2 mg kg^{-1}). Conversely, average concentrations of As, Pb, Cr and Zn are within or below the majority of established guideline levels.

Figure 6 illustrates a comparative study of the ore-derived anomaly: Copper (mean ≈ 754 mg kg^{-1}) and Molybdenum (≈ 67 mg kg^{-1}) are significantly raised over global background levels, while Arsenic (≈ 12 mg kg^{-1}) and Cobalt (≈ 19 mg kg^{-1}) are notably higher than background levels (~4.7 and ~6.9 mg kg^{-1}, respectively). Conversely, Cr (≈ 36.6 mg kg^{-1}), V (≈ 65.8 mg kg^{-1}) and Zn (≈ 55.5 mg kg^{-1}) correspond more closely to crustal averages. Bulk Fe averages roughly 2.9 wt% (≈ 28,975 mg kg^{-1}), which is below the normal global proxy of around 4.7 wt%, indicating that the potential hazard is not primarily influenced by iron but is instead linked to trace-element enrichment resulting from mining and processing activities. These totals require a comprehensive analysis of chemical speciation, which is crucial for understanding mobility and health implications.

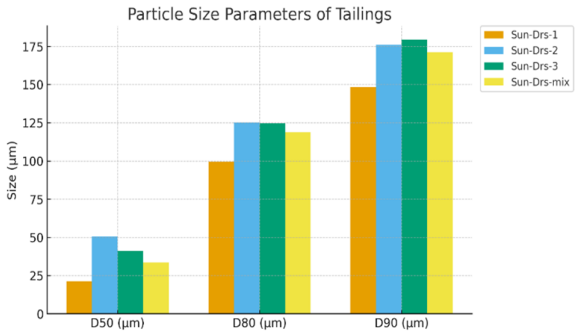

Figure 5. Particle size parameters (D50, D80, D90) showing fine textures that enhance reactivity and dust-related exposure potential.

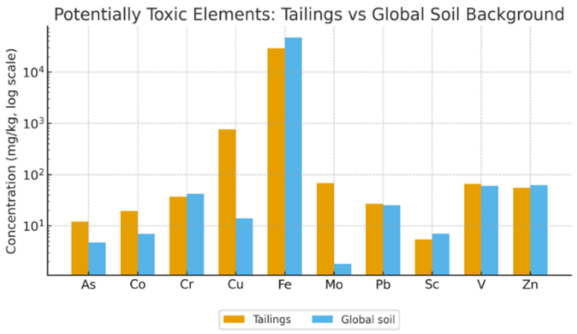

Figure 6. Mean PTE concentrations in tailings versus global soil background (log scale). Cu and Mo dominate the anomaly, reflecting porphyry-ore residue.

The essential statistical properties of these elements (Table 4) form the foundation for subsequent investigations. Iron (Fe) and copper (Cu) are predominant, with average concentrations of approximately 28,975 mg kg^{-1} and 753.8 mg kg^{-1}, respectively. Both elements exhibit minimal relative variability (CV = 0.034 for Fe; CV ≈ 0.086 for Cu), suggesting homogeneous distributions throughout the sampled material. Arsenic (As) demonstrates the highest heterogeneity (CV = 0.262) and significant right skewness (skewness ≈ 1.127), indicating the presence of localized hotspots with relation to the median. Cobalt (Co), scandium (Sc), molybdenum (Mo) and vanadium (V) exhibit minimal coefficients of variation (about 0.038, 0.039, 0.042 and 0.045, respectively), with scandium nearing complete symmetry.

Table 4. Descriptive statistics of elemental concentrations (mg/kg) in tailings samples and comparison with soil quality guideline thresholds.

Statistics	As	Co	Cr	Cu	Fe	Mo	Pb	Sc	V	Zn
Mean	12.025	19.3	36.625	753.75	28975	67.4	26.75	5.35	65.75	55.5
Median	11.4	19.35	36.35	759	29100	67.15	26.5	5.35	66	54.5
Std. Deviation	3.14682	0.72572	2.33292	64.79905	974.2519	2.81306	2.75379	0.20817	2.98608	3.10913
Skewness	1.127	-0.345	0.569	-0.352	-0.223	0.364	0.323	0	-0.423	1.597
CV	0.262	0.038	0.064	0.086	0.034	0.042	0.103	0.039	0.045	0.056
Kurtosis	2.208	-0.577	-0.601	-1.806	-4.726	-2.195	-3.033	0.391	-0.416	2.704
Minimum	8.9	18.4	34.2	675	27900	64.5	24	5.1	62	53
Maximum	16.4	20.1	39.6	822	29800	70.8	30	5.6	69	60
Global Soil	4.7	6.9	42	14	47000	1.8	25	7	60	62
ISQG (Iran)	18	40	110	100		10	80		100	200
ChSQG (China)	30		200	100			300			250
CSQG (Canada)	12	15	87	91		2	600		130	360
DSQG (Netherlands)	29	9	100	36			85			140

Figure 7 presents histograms with kernel-density overlays for As, Co, Cr, Cu, Fe, Mo, Pb, Sc, V and Zn, complementing the summary data presented in Table 4. The distributional profiles validate the descriptive metrics: As and Zn demonstrate a slight right skew, Cu has a higher dispersion around a pronounced central tendency, whereas Fe is quite tightly grouped. In contrast, Co, Sc, Mo and V exhibit narrow distributions indicative of low coefficients of variation, with Sc nearing symmetry. Collectively, these diagnostics offer a visual assessment of normalcy and possible outliers before the ensuing correlation and clustering investigations.

Figure 7. Distributions of elemental concentrations (As, Co, Cr, Cu, Fe, Mo, Pb, Sc, V, Zn) in Sungun tailings. Each panel shows a histogram with a kernel-density estimate.

3.2. Assessment of Contamination and Geochemical Associations

The geochemical data were further interpreted using environmental indices and statistical analyses to quantify the degree of contamination and to elucidate the relationships and common sources among the elements.

3.2.1. Elemental Enrichment and Contamination Levels

The Enrichment Factor (EF) was determined for each element to differentiate between those originating from natural geogenic sources and those concentrated by anthropogenic activities, utilizing scandium (Sc) as a conservative normalizing element of crustal origin. The findings of this investigation are displayed in Fig. 8. The EF values indicate a clear hierarchy of pollution. Copper and molybdenum demonstrate "extremely high enrichment," with average enrichment factor values of roughly 70 and 49, respectively. This signifies that their concentrations in the tailings much exceed those expected from natural crustal sources alone. Arsenic and cobalt exhibit "moderate enrichment" ($2 \leq EF < 5$), signifying a

notable yet less pronounced concentration over baseline values. Conversely, elements including chromium, iron, lead, vanadium and zinc possess EF values under 2, categorizing them as exhibiting "minimal enrichment".

This approach offers clear quantitative evidence of the human-induced effects of mining and mineral processing on the surrounding ecosystem. The exceptionally elevated EFs for Cu and Mo unequivocally indicate that their existence is predominantly attributable to the mining activity, given they were the targeted commodities. The considerable enrichment of arsenic and cobalt indicates a significant geochemical correlation with the copper mining process; they were probably concentrated as accessory minerals in conjunction with the primary ore. The modest enrichment of the residual elements indicates that they are predominantly linked to the natural host rock (gangue) and have not been substantially concentrated via the ore beneficiation process. The EF analysis effectively disaggregates the intricate geochemical signature of the tailings into a significant, anthropogenic, ore-related component (Cu, Mo, As, Co) overlaying a background, geogenic, host-rock signature.

Figure 8 presents box plots (logarithmic scale) of enrichment factors (EF) for the four samples, including individual data points and a line representing the mean. Copper (mean enrichment factor = 70.7, range 60–80) and molybdenum (≈ 49.1, range 44.8–54.0) exhibit significant enrichment (≫ 40), signifying anthropogenic accumulation in ore residues. Arsenic (mean ≈ 3.3, range 2.6–4.5) and cobalt (≈ 3.7, range 3.5–3.9) are categorized within the 2–5 "considerable" range, while chromium, iron, lead, vanadium and zinc are grouped near unity (∼ 1–1.4), aligning with lithogenic background levels. This EF structure differentiates ore-metal signals from background noise, corroborates the observed Cu–Mo co-enrichment and warns that totals alone may mislead environmental significance if speciation is neglected.

3.2.2. Statistical Analysis and Inter-Element Relationships

A Pearson correlation analysis was conducted to examine the geochemical affinities and putative shared sources among the elements, with the findings presented in Figure 9. A hierarchical cluster analysis, illustrated as a dendrogram, was utilized to classify items based on their statistical associations (Figure 10). The results indicate two principal and predominantly opposing, groups of constituents within the tailings.

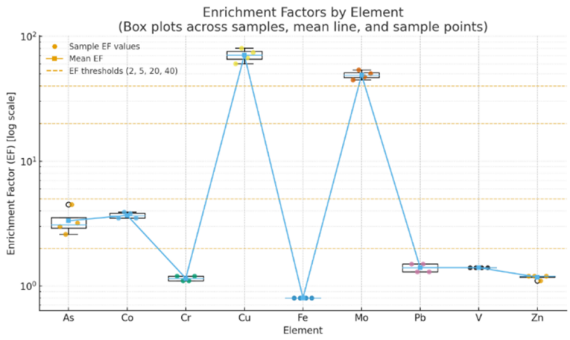

Figure 8. Box plots (log scale) of enrichment factors (EF) across four samples, with points for individual values and a line for means.

The primary category pertains to the ore-related association, characterized by a strong positive correlation between Cu and MO. This robust statistical correlation validates their close geochemical relationship, stemming from the identical porphyry ore body from which they were co-precipitated from hydrothermal fluids, presumably as chalcopyrite and molybdenite. The second group comprises the gangue-related elements, which include Cr, Pb, Sc, V and Zn. These elements exhibit strong positive correlations, indicating a common origin and similar activity within the tailings system. This signature reflects the host rock matrix (gangue minerals) that was processed with the ore. These elements are predominantly lithophilic or associated with small, non-target sulfide minerals dispersed within the bulk rock mass. Iron (Fe) exhibits alignment with the lithogenic association, demonstrating positive correlations with the Cr–Pb–Sc–V–Zn cluster, while displaying negative correlations with Cu and Mo, so underscoring its affinity for the gangue matrix rather than the ore phase.

A significant discovery is the robust and constant negative association between the ore-associated group (Cu, Mo) and the gangue-associated group (Cr, Pb, Sc, V, Zn). This adversarial relationship indicates that the tailings are not a chemically uniform substance, but rather a heterogeneous physical amalgamation of at least two separate geochemical particle populations. Sections of the tailings rich in residual ore particles (high in Cu and Mo) are inherently lacking in gangue-signature elements and conversely. The variability significantly impacts environmental management and potential reprocessing solutions, as the environmental risk and economic

opportunity are inequitably allocated throughout the tailings mass.

The correlation architecture depicted in Figure 9 demonstrates coherent relationships aligned with mineralogical partitioning. The Cu–Mo pair exhibits a significant positive correlation ($r \approx 0.98$), indicating their simultaneous presence in sulfide hosts; the Cr–Pb–Sc–V–Zn elements constitute a lithogenic/oxyhydroxide cluster with robust internal associations (e.g., Cr–Pb $r \approx 0.93$, Pb–Sc $r \approx 0.99$, V–Sc $r \approx 0.99$). Cu and Mo have a substantial anti-correlation with Cr, V, Sc and Pb (e.g., Cu–Cr $r = -0.84$, Co–Fe $r \approx -0.81$), suggesting the presence of different particle populations. These patterns suggest that redox alterations would induce varying release behaviours among groups of elements and necessitate a speciation-first assessment of mobility.

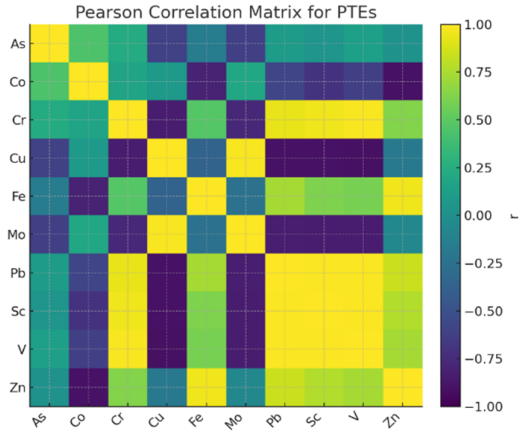

Figure 9. Pearson correlation heatmap for PTEs. Cu–Mo correlate strongly, while Cr–Pb–Sc–V–Zn form a lithogenic cluster inversely related to ore metals.

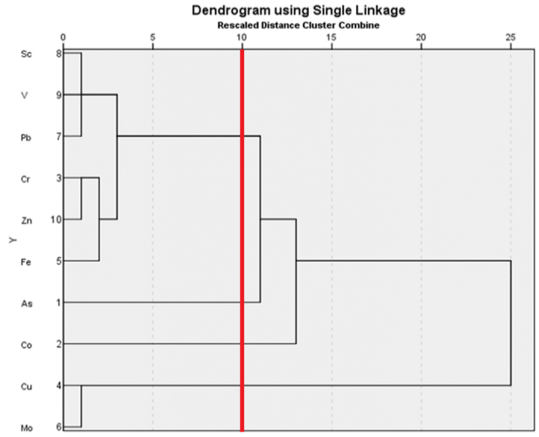

Figure 10. Dendrogram of elements using single linkage clustering. The red line at rescaled distance 10 indicates the cut-off, dividing the data into distinct clusters of associated elements.

3.3. Geochemical Fractionation and Potential Mobility of PTEs

The evaluation of total elements concentrations and enrichment factors is crucial for preliminary site assessment and recognizing primary anthropogenic pollutants; nevertheless, these metrics are inadequate for a precise evaluation of environmental risk. The toxicity, mobility and final bioavailability of an element are determined not by its overall quantity but by its particular chemical form and solid-phase interaction within the tailings matrix. A modified BCR sequential extraction approach was utilized to clarify these essential features. This well recognized method operationally delineates the partitioning of PTEs into fractions of differing lability, offering a better mechanistic foundation for assessing their potential for environmental release and associated health hazards.

3.3.1. Distribution of PTEs in Geochemical Fractions

The BCR protocol partitions elements into four operationally defined geochemical fractions, each susceptible to mobilization under different environmental conditions. The fractions are as follows: F1, the acid-soluble/exchangeable fraction, deemed immediately bioavailable; F2, the reducible fraction, consisting of elements bound to Fe-Mn oxyhydroxides, stable under oxidizing conditions but mobile under reducing (anoxic) conditions; F3, the oxidizable fraction, comprising elements linked to sulfide minerals and organic matter, stable under reducing conditions but releasing their contents upon oxidation; and R, the residual fraction, where elements are structurally integrated into the crystalline lattice of silicate minerals, regarded as immobile except under extreme weathering conditions.

The sequential extraction data, displayed in Table 5, demonstrate clear partitioning patterns for the PTEs, which are closely associated with the established mineralogy of the Sungun tailings. The recovery rates, derived from the comparison of the total of the four fractions to the pseudo-total concentration established after acid digestion, were predominantly exceptional (range from 94% to 111%), so affirming the effectiveness and mass balance of the extraction method for this particular material.

Table 5. Geochemical Fractionation of PTEs in Sungun Tailings. Values represent the mean of four analyses. F1: Acid-Soluble/Exchangeable; F2: Reducible; F3: Oxidizable; R: Residual. Recovery (%) = × 100.

PTE	F1	F2	F3	R	Total	Recovery (%)	F1 (%)	F2 (%)	F3 (%)	R (%)
Co	1.2	3.5	5.5	8.7	19.3	98	6.3	18.5	29.1	46.0
Cr	2.2	1.6	6.1	29.2	36.6	107	5.6	4.1	15.6	74.7
Cu	58.4	94.3	404.3	202.8	753.8	101	7.7	12.4	53.2	26.7
Fe	184.1	1632.8	283.2	26411.3	28975	98	0.6	5.7	1.0	92.6
Mo	4.3	8.1	28.7	33.5	67.4	111	5.8	10.9	38.5	44.9
Pb	4.0	6.2	10.0	8.5	26.8	107	14.0	21.7	34.8	29.6
Sc	1.3	1.0	1.1	3.0	5.4	119	20.3	15.6	17.2	46.9
V	6.7	8.0	3.7	49.8	65.8	104	9.8	11.7	5.4	73.0
Zn	8.4	26.9	4.8	19.5	55.5	107	14.1	45.2	8.1	32.7

The partitioning patterns provide direct chemical evidence of the host phases for the key elements of concern:

Copper (Cu) and Molybdenum (Mo): The primary economic metals exhibit a clear association with the mobile fractions. A striking 53.2% of the total copper is found in the oxidizable fraction (F3), with another 20.1% in the acid-soluble and reducible fractions (F1+F2). This provides unambiguous evidence that a substantial portion of the highly enriched copper persists as residual sulfide minerals (e.g., chalcopyrite), which are susceptible to release under the oxidizing conditions prevalent in the upper layers of a tailings facility. Molybdenum shows a similar, though less pronounced, trend with 38.5% in the oxidizable fraction. This indicates that the principal long-term environmental threat from the tailings is the potential for AMD-driven release of these sulfide-bound metals.

Vanadium (V), Chromium (Cr) and Iron (Fe): In stark contrast, these lithophilic elements are overwhelmingly concentrated in the residual (R) fraction, with 73.0%, 74.7% and 92.6% of their total mass, respectively, being structurally bound within the silicate mineral matrix. This finding is consistent with their geogenic origin and incorporation into the lattice of gangue minerals such as feldspars, micas and pyroxenes, which were identified by XRD analysis. The low proportion of these elements in the mobile fractions signifies their very low mobility and bioavailability under typical environmental conditions, a critical finding for the subsequent health risk assessment.

Zinc (Zn), Lead (Pb) and Cobalt (Co): These elements display a more distributed profile, indicating multiple host phases and a higher potential for mobility. Zinc is predominantly found in the reducible fraction (F2, 45.2%), suggesting its strong association with secondary Fe-Mn oxyhydroxide coatings on mineral grains. Lead is partitioned significantly across the reducible (F2, 21.7%) and oxidizable (F3, 34.8%) fractions, consistent with its association with both secondary iron oxides and accessory sulfide minerals like galena. These distributions imply that the mobility of Zn and Pb is highly sensitive to changes in both redox potential and pH.

The BCR fractionation depicted in Figure 11 illustrates that host-phase controls take precedence over total values. Cu is predominantly oxidizable, with F3 approximately 53%, F2 approximately 12% and F1 around 8%; Mo similarly concentrates in F3 at approximately 39% and F2 at approximately 11%. Zn is primarily reducible (F2 ≈ 45%), indicative of Fe–Mn oxyhydroxide sorption. Conversely, Fe (R ≈ 93%), Cr (R ≈ 75%) and V (R ≈ 73%) are predominantly residual and immobile at near-surface conditions. Lead (Pb) is combined with F3 (about 35%), F2 (approximately 22%) and R (approximately 30%), indicating partial lability. These patterns indicate that short- to medium-term release is regulated by redox-sensitive hosts (sulfidic/oxyhydroxide) rather than overall stockpiles.

3.3.2. Mobility and Bioavailability Assessment

The fractionation data can be converted into a direct evaluation of environmental risk by calculating the overall mobility of each element. The "mobile fraction" is defined as the sum of the first three fractions (F1+F2+F3), representing the portion of the total elemental load that is not structurally locked within the silicate matrix and is therefore potentially available for environmental transport and biological uptake. A Mobility Factor (MF) was computed for each PTE to enable comparison ranking. Figure 12 delineates the ranking of mobility, expressed as MF (%), for several elements: Cu (73.3) > Pb (70.4) > Zn (67.3) > Mo (55.1) ≈ Co (54.0) ≈ Sc (53.1) ≫ V (26.9) ≈ Cr (25.3). Consequently, elements linked to oxidizable or reducible phases predominate in the

bioavailable pool, while residual-dominated vanadium and chromium demonstrate restricted short-term mobility. This ranking alters the focus suggested by totals and offers a quantitative link to exposure evaluation, especially ingestion, which is affected by the fine, labile fractions.

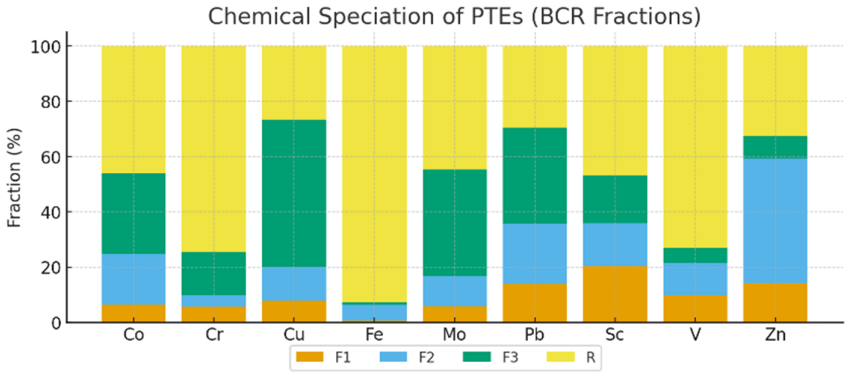

Figure 11. BCR fractionation (F1– F3 + Residual) as % of total for key PTEs, highlighting labile hosts (Cu/Mo/Zn) versus residual (V/Cr/Fe).

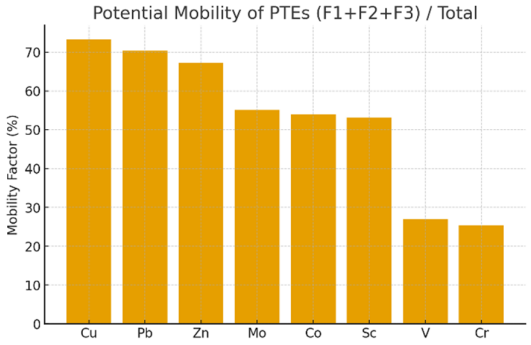

Figure 12. Mobility Factor (%) computed from mobile fractions (F1+F2+F3). Cu, Pb and Zn are predominantly labile; V and Cr are mostly immobile.

The mobility evaluation indicates a risk hierarchy that fundamentally differs from that based just on total concentrations or enrichment factors. Copper exhibits the greatest potential mobility (MF = 73.3%), after by lead (70.4%) and zinc (67.3%). This signifies that, although their overall concentrations are smaller than those of copper, these elements largely exist in labile forms and provide a substantial and immediate environmental hazard. In contrast, the elements principally linked to the gangue mineralogy in the statistical study, vanadium (MF = 26.9%) and chromium (MF = 25.3%), have the least mobility. This indicates that despite their significant total concentration, the majority of their mass is confined to non-bioavailable forms. This discovery directly confronts a significant weakness of depending exclusively on total concentration data for risk assessment, as emphasized in the introduction and requires a reassessment of human health risks utilizing these more realistic, bioavailability-based exposure concentrations.

3.4. Human Health Risk Assessment (HHRA)

The results of the bioavailability-corrected HHRA, summarized in Table 6, indicate a significant shift in the risk profile of the tailings compared to the initial assessment based on total concentrations. The total non-carcinogenic risk for children, expressed as the Hazard Index (HI), is calculated to be 2.04. While this value is substantially lower than the 5.78 derived from total concentrations, it remains above the safe threshold of 1.0, indicating that a potential for adverse non-carcinogenic health effects for children persists. For adults, the total HI is 0.48, a value well below the threshold of 1.0. This is a crucial assessment, indicating that under the simulated exposure scenario, the tailings do not present a substantial non-carcinogenic danger to the adult population.

Ingestion remains the dominant exposure pathway, contributing over 98% of the total risk for both receptor groups. A detailed analysis of the elemental contributions to the HI for children reveals a fundamental rebalancing of risk. Vanadium (V), previously recognized as the predominant hazard, now yields a Hazard Index (HI) of 1.26. While it remains the single largest contributor and its HQ is still above the safe level of 1.0, its dominance is drastically reduced. The next largest contributors are Copper (Cu) with an HI of 0.35, followed by Chromium (Cr) at 0.21. This indicates that the significant danger initially associated with vanadium was a byproduct of its elevated toxicity value coupled with a total concentration that did not accurately reflect its low

bioavailability (27% mobile). The speciation analysis provides a more accurate picture, showing a moderate but clear risk driven primarily by bioavailable vanadium.

The assessment of carcinogenic risk (CR) remains unchanged in its conclusion. The calculated total CR values for both children (2.1×10^{-7}) and adults (1.9×10^{-7}) are several orders of magnitude below the commonly accepted regulatory threshold range of 1×10^{-6} to 1×10^{-4}. Therefore, the tailings do not pose a significant carcinogenic risk under the assumed exposure conditions.

Table 6. Summary of Bioavailability-Corrected Non-Carcinogenic (HI) and Carcinogenic (CR) Health Risk Indices for Children and Adults via Different Exposure Pathways.

Receptor	Risk Index	Ingestion	Dermal Contact	Inhalation	Total Risk
Child	HI (non-carcinogenic)	2.01	0.03	<0.001	2.04
	CR (carcinogenic)	1.8×10−7	2.8×10−8	1.1×10−11	2.1×10−7
Adult	HI (non-carcinogenic)	0.47	<0.01	<0.001	0.48
	CR (carcinogenic)	1.6×10−7	2.6×10−8	2.2×10−11	1.9×10−7

Figure 13 illustrates that intake predominantly influences non-carcinogenic risk for both receptors, with the kid hazard index (HI) around 2.01 surpassing unity, while the adult HI is approximately 0.47, remaining below the threshold. Dermal contributions are minimal (child ~0.03; adult ~0.01) and inhalation is insignificant at the assessed conditions. The allocation of pathways aligns with the previously established fine particle sizes and bioavailable fractions, emphasizing ingestion-centric strategies (soil/dust management, hygiene treatments) for risk mitigation.

To better understand which elements drive the overall non-carcinogenic risk for children, the Hazard Index (HI) was decomposed into contributions from individual elements based on their bioavailable concentrations. The results reveal that vanadium (V) is the dominant contributor, with an HI of approximately 1.26 exceeding the threshold value of 1.0 on its own. This increased contribution is not only dependent on total concentration but rather indicates vanadium's considerable toxicity (low RfD) coupled with its moderate bioavailability (≈27% of total). Copper (Cu) and chromium (Cr) represent the next most significant contributors, with HI values of 0.35 and 0.21 respectively, followed by lead (Pb), zinc (Zn), molybdenum (Mo), cobalt (Co) and arsenic (As), all of which contribute comparatively minor fractions to the cumulative risk. The pattern emphasizes that risk prioritization should rely on speciation-corrected bioavailable fractions instead of total concentrations, since total values would exaggerate the significance of V while underestimating that of Cu and Pb. Figure 14 graphically highlights this distribution, making clear that targeted management strategies aimed at reducing vanadium bioavailability would yield the greatest reduction in overall child health risk.

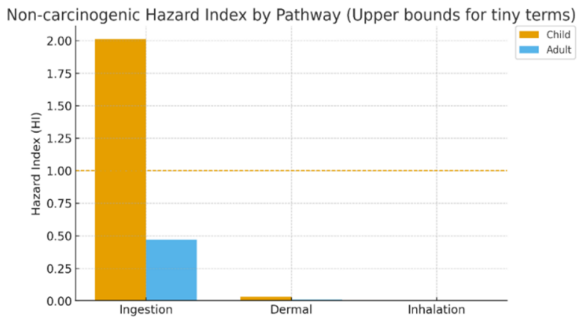

Figure 13. Non-carcinogenic Hazard Index (HI) partitioned by pathway for child and adult receptors. Dashed line marks HI = 1.

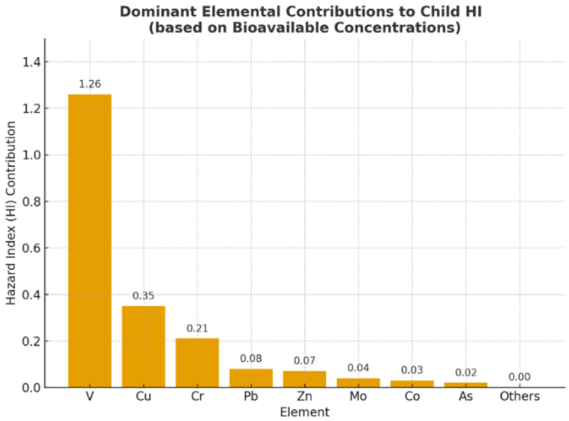

Figure 14. Dominant elemental contributions to the non-carcinogenic Hazard Index (HI) for children, calculated using bioavailable (F1+F2+F3) concentrations.

3.5. Limitations and Strengths of the Study

This study utilized a speciation-based methodology to evaluate health hazards instead than depending exclusively on total elements concentrations. Given that elements occur in different geochemical phases and their chemical mobility varies across these phases, applying a speciation framework is essential for accurately evaluating potential health impacts. Nevertheless, the present study has several limitations that should be considered in future research. Due to financial constraints, only three sampling stations were included. Due to financial constraints, only three sampling stations were selected in this study. It is important to highlight that the total number of samples studied was 20, as each geochemical phase derived from the sequential extraction technique constitutes an individual chemical analysis. All samples were consistently used for mineralogical characterization, particle-size analysis, total concentration measurement and sequential extraction, which collectively resulted in substantial analytical costs.

It Is also Important to highlight that the composite samples Indicated minimal variation among the sampling stations. This suggests that increasing the number of sampling locations would not significantly alter the overall research findings. Nonetheless, for more robust geostatistical and multivariate analyses, future studies would benefit from incorporating a larger number of sampling stations although this would require considerable additional funding.

4. Conclusions

This study presents a comprehensive assessment of environmental and human health risks associated with tailings from the Sungun porphyry copper mine, emphasizing the limitations of relying solely on total elemental concentrations. By integrating physicochemical, mineralogical and geochemical analyses with chemical speciation, the research provides a mechanistic understanding of pollutant behavior and associated risks. The tailings exhibit a persistent acid-generating potential, as pyrite (~4%) exceeds the neutralizing capacity of calcite (~2%), indicating insufficient buffering against acid mine drainage. The samples have a distinct anthropogenic geochemical signature, characterized by significant enrichment of copper and molybdenum, alongside modest enrichment of arsenic and cobalt, indicative of the effects of mining and processing operations. Chemical speciation analysis revealed that elements such as copper, lead, zinc and molybdenum are largely bioavailable, while vanadium and chromium are predominantly immobile, demonstrating that total concentrations can overestimate environmental and health risks. Incorporation of bioavailability into human health risk assessment revealed that children face non-carcinogenic risks, primarily due to vanadium, whereas adult risks and carcinogenic hazards for both groups remain within acceptable limits. The findings highlight the critical importance of a speciation-based approach for accurately evaluating the environmental behaviour and health risks of mine tailings, providing a robust foundation for informed management and remediation strategies.

References

[1]. Cacciuttolo, C., Cano, D., & Custodio, M. (2023). Socio-Environmental Risks Linked with Mine Tailings Chemical Composition: Promoting Responsible and Safe Mine Tailings Management Considering Copper and Gold Mining Experiences from Chile and Peru. *Toxics, 11*.

[2]. Wang, P., Sun, Z., Hu, Y., & Cheng, H. (2019). Leaching of heavy metals from abandoned mine tailings brought by precipitation and the associated environmental impact. *Science of the total environment, 695,* 133893.

[3]. Rubinos, D., Jerez, Ó., Forghani, G., Edraki, M., & Kelm, U. (2021). Geochemical stability of potentially toxic elements in porphyry copper-mine tailings from Chile as linked to ecological and human health risks assessment. *Environmental Science and Pollution Research, 28,* 57499 - 57529.

[4]. Kerfoot, W., Swain, G., Regis, R., Raman, V., Brooks, C., Cook, C., & Reif, M. (2025). Coastal Environments: LiDAR Mapping of Copper Tailings Impacts, Particle Retention of Copper, Leaching and Toxicity. *Remote Sensing*.

[5]. Hassanzad, S., Pirkharrati, H., Ahangari, M., & Asadzadeh, F. (2024). Assessment of the potential environmental effects of newly deposited mine tailings from the Sungun Copper mine. Iranian Journal of Health and Environment, 17(1), 139–162.

[6]. Alizadeh, A., Ghorbani, J., Motamedi, J., Vahabzadeh, G., van der Ent, A., & Edraki, M. (2024). Soil contamination around porphyry copper mines: an example from a semi-arid climate. *Environmental Monitoring and Assessment, 196 (2),* 204.

[7]. Moore, F., & Aghazadeh, A. A. (2012). Trace metal occurrence and mobility assessment in stream sediments near the Sungun porphyry copper deposit in northwest Iran. *Mine Water and the Environment, 31 (1),* 29–39.

[8]. Villegas, C., & Zagury, G. (2023). Incorporating oral, inhalation and dermal bioaccessibility into human health risk characterization following exposure to Chromated Copper Arsenate (CCA)-contaminated soils. *Ecotoxicology and environmental safety, 249,* 114446.

[9]. Perrotta, B. G., Kidd, K. A., Campbell, K. M., Croteau, M.-N., Kane, T. J., Marcarelli, A. M., Blaine McCleskey, R., Paterson, G., Stricker, C. A., & Walters, D. M. (2025). Metal-rich lacustrine sediments from legacy mining perpetuate copper exposure to aquatic-riparian food webs. *Integrated Environmental Assessment and Management, 21 (2),* 414–424.

[10]. Xiao, M., Xu, S., Yang, B., Zeng, G., Qian, L., Huang, H., & Ren, S. (2022). Contamination, source apportionment and health risk assessment of heavy metals in farmland soils surrounding a typical copper tailings pond. *International Journal of Environmental Research and Public Health, 19(21),* 14264.

[11]. Shetty, R., Jagadeesha Pai1, B., Salmataj, S., & Naik, N. (2024). Assessment of Carcinogenic and non-carcinogenic risk indices of heavy metal exposure in different age groups using Monte Carlo Simulation Approach. Scientific Reports, 14.

[12]. Moreno-Rodríguez, V., Del Rio-Salas, R., Loredo-Portales, R., Núñez-Ibarra, H. D., Romo-Morales, D., Pi-Puig, T., & García-Martínez, D. (2024). Urban mine tailings and efflorescent crusts: unveiling health implications in Nacozari de García, Mexico. *Environmental Earth Sciences, 83(3),* 116.

[13]. Akhavan, A., & Golchin, A. (2024). Health risk assessment of lead-zinc mine tailing in Angoran, Zanjan, Iran. *Environmental Quality Management, 33(3),* 141–155.

[14]. Fry, K. L., Wheeler, C. A., Gillings, M. M., Flegal, A. R., & Taylor, M. P. (2020). Anthropogenic contamination of residential environments from smelter As, Cu and Pb emissions: Implications for human health. *Environmental Pollution, 262,* 114235.

[15]. Diaby, N., Dold, B., Rohrbach, E., Holliger, C., & Rossi, P. (2015). Temporal evolution of bacterial communities associated with the in situ wetland-based remediation of a marine shore porphyry copper deposit. *Science of the Total Environment, 533,* 110–121.

[16]. Nasrabadi, T., Nabi Bidhendi, G. R., Karbassi, A. R., Hoveidi, H., Nasrabadi, I., Pezeshk, H., & Rashidinejad, F. (2009). Influence of Sungun copper mine on groundwater quality, NW Iran. *Environmental Earth Sciences, 58,* 693–700.

[17]. Hezarkhani, A., Williams-Jones, A. & Gammons, C. (1999). Controls of alteration and mineralization in the Sungun porphyry copper deposit, Iran; evidence from fluid inclusions and stable isotopes. *Economic Geology, 93,* 651-670.

[18]. Kamali, A., Moayyed, M., Amel, N., Mohammad, F., Brenna, M., Saumur, B., & Santos, J. (2020). Mineralogy, mineral chemistry and thermobarometry of post-mineralization dykes of the Sungun Cu–Mo porphyry deposit (Northwest Iran). *Open Geosciences, 12,* 764 - 790.

[19]. Hassanpour, S., Senemari, S., & Roomi, N. (2022). Delineation of mineralization zones by multivariate fractal and zonality modeling in south of the Sungun and Kighal porphyry systems, NW, Iran. *Arabian Journal of Geosciences, 15.*

[20]. Sohrabian, B., & Tercan, A. E. (2025). Grade Estimation Through the Gaussian Copulas: A Case Study. *Journal of Mining and Environment, 1(16),* 1-13.

[21]. Simmonds, V., Moazzen, M., & Mathur, R. (2017). Constraining the timing of porphyry mineralization in northwest Iran in relation to Lesser Caucasus and Central Iran; Re–Os age data for Sungun porphyry Cu–Mo deposit. *International Geology Review, 59(12),* 1561–1574.

[22]. Keshavarzi, B., Najmeddin, A., Moore, F., & Afshari Moghaddam, P. (2019). Risk-based assessment of soil pollution by potentially toxic elements in the industrialized urban and peri-urban areas of Ahvaz metropolis, southwest of Iran. *Ecotoxicology and Environmental Safety, 167,* 365-375.

[23]. Kabata-Pendias, A. (2010). Trace Elements in Soils and Plants (4th ed.). *CRC Press.*

[24]. U.S. EPA. (2015, September 10). Regional Screening Levels (RSLs) - User's Guide. Www.epa.gov. https://www.epa.gov/risk/regional-screening-levels-rsls-users-guide.

[25]. U.S. EPA. (2011). Exposure Factors Handbook: U.S. Environmental Protection Agency, Washington, DC, EPA/600/R-09/052F.

انجمن مهندسی معدن ایران
نشریه مهندسی معدن و محیط زیست
نشانی نشریه: www.jme.shahroodut.ac.ir
دانشگاه صنعتی شاهرود

گونه‌پذیری زمین‌شیمیایی، میزان آلودگی و ارزیابی خطر سلامت ناشی از عناصر بالقوه سمی در باطله‌های معدن مس پورفیری سونگون

علی نجم‌الدین*، طاها صلاحجو و کیمیا زنده‌دل

دانشکده مهندسی معدن، دانشکدگان فنی، دانشگاه تهران، تهران، ایران

اطلاعات مقاله

تاریخ ارسال: ۲۰۲۵/۱۱/۱۵

تاریخ داوری: ۲۰۲۵/۱۱/۲۶

تاریخ پذیرش: ۲۰۲۶/۰۱/۱۹

DOI: 10.22044/jme.2026.17152.3391

کلمات کلیدی

باطله‌های معدنی
ارزیابی خطر سلامت
گونه‌پذیری شیمیایی
معدن سونگون

چکیده

استخراج مس پورفیری مقادیر قابل‌توجهی باطله تولید می‌کند که به دلیل توانایی در تولید اسید و آزادسازی عناصر بالقوه سمی، مخاطرات جدی زیست‌محیطی و بهداشتی برای انسان به همراه دارد. در این مطالعه، ارزیابی یکپارچه‌ای از ریسک‌های زیست‌محیطی و سلامت انسانی ناشی از باطله‌های معدن مس پورفیری سونگون در شمال‌غرب ایران ارائه شده است. بدین منظور، رویکردی جامع و میان‌رشته‌ای به کار گرفته شد که شامل ترکیب آنالیزهای فیزیکوشیمیایی، کانی‌شناسی و ژئوشیمیایی با روش‌های آماری بود. گونه‌بندی شیمیایی عناصر با استفاده از روش اصلاح‌شده پیشنهادی دفتر مرجع جامعه اروپا انجام شد؛ روشی که در مطالعات متعدد برای ارزیابی تفکیک ژئوشیمیایی و تحرک‌پذیری عناصر به کار رفته است. هدف اصلی این پژوهش، گذار از تحلیل صرف غلظت کل عناصر به سوی ارزیابی دقیق‌تر ریسک مبتنی بر زیست‌دسترس‌پذیری، با بهره‌گیری از چارچوب سازمان حفاظت محیط‌زیست ایالات متحده برای کودکان و بزرگسالان بود. بررسی‌های کانی‌شناسی نشان داد که باطله‌ها دارای پتانسیل خالص تولید اسید هستند، به‌گونه‌ای که مقدار پیریت (حدود ۴ درصد) معمولاً بیش از کانی خنثی‌کننده اصلی، یعنی کلسیت (حدود ۲ درصد)، است. نتایج آنالیزهای ژئوشیمیایی بیانگر غنی‌شدگی قابل‌توجه مس و مولیبدن و همچنین غنی‌شدگی متوسط آرسنیک و کبالت در باطله‌ها بود. در میان عناصر مورد بررسی، بیشترین ضرایب تحرک به ترتیب متعلق به مس (۸۱٫۴۹٪)، سرب (۷۶٫۷۱٪)، روی (۷۱٫۶۵٪) و مولیبدن (۵۹٫۲۷٪) بود. شاخص خطر غیرسرطان‌زایی برای کودکان برابر با ۲٫۰۴ به‌دست آمد که از حد ایمنی فراتر است و در این میان، وانادیم زیست‌دسترس‌پذیر به‌عنوان عامل اصلی ریسک شناسایی شد. این یافته‌ها نشان می‌دهد که اتکای صرف بر غلظت کل عناصر بالقوه سمی می‌تواند گمراه‌کننده باشد و بر ضرورت انجام ارزیابی‌های مبتنی بر گونه‌پذیری شیمیایی برای توصیف دقیق رفتار زیست‌محیطی و مخاطرات سلامت ناشی از باطله‌های معدنی تأکید می‌کند.

نویسنده مسئول مکاتبات: najmeddinali@ut.ac.ir (ع. نجم‌الدین)